Engineering pressure retarded osmosis membrane bioreactor (PRO-MBR) for simultaneous water and energy recovery from municipal wastewater

Shuyue Liu[a], Weilong Song[a,*], Manli Meng[a], Ming Xie[b], Qianhong She[c], Pin Zhao[a], Xinhua Wang[a]

[a] Jiangsu Key Laboratory of Anaerobic Biotechnology, School of Environmental and Civil Engineering, Jiangnan University, Wuxi 214122, PR China

[b] Department of Chemical Engineering, University of Bath, Bath, BA2 7AY, UK

[c] School of Civil and Environmental Engineering, Nanyang Technological University, Singapore 639798, Singapore

*Corresponding author:

Tel:+86-13081495594, Email: swl@jiangnan.edu.cn (W. Song)

Abstract

Osmotic membrane bioreactors (OMBR) have gained increasing interest in wastewater treatment and reclamation due to their high product water quality and fouling resistance. However, high energy consumption (mostly by draw solution recovery) restricted the wider application of OMBR. Herein, we propose a novel pressure retarded osmosis membrane bioreactor (PRO-MBR) for improving the economic feasibility. In comparison with conventional FO-MBR, PRO-MBR exhibited similar excellent contaminants removal performance and comparable water flux. More importantly, a considerable amount of energy can be recovered by PRO-MBR (4.1 kWh/100 $m^2 \cdot d$), as a result of which, 10.02% of the specific energy consumption (SEC) for water recovery was reduced as compared with FO-MBR (from 1.42 kWh/m^3 to 1.28 kWh/m^3). Membrane orientation largely determined the performance of PRO-MBR, higher power density was achieved in AL-DS orientation (peak value of 3.4 W/m^2) than that in AL-FS orientation (peak value of 1.4 W/m^2). However, PRO-MBR suffered more severe and complex membrane fouling when operated in AL-DS orientation, because the porous support layer was facing sludge mixed liquor. Further investigation revealed fouling was mostly reversible for PRO-MBR, it exhibited similar flux recoverability (92.4%) to that in FO-MBR (95.1%) after osmotic backwash. Nevertheless, flux decline due to membrane fouling is still a restricting factor to power generation of PRO-MBR, its power density was decreased by 38.2% in the first 60 min due to the formation of fouling. Overall, in perspective of technoeconomic feasibility, the PRO-MBR demonstrates better potential than FO-MBR in wastewater treatment and reclamation

and deserves more research attention in the future.

Keywords: pressure retarded osmosis; forward osmosis; membrane bioreactor; energy recovery; wastewater treatment

1. Introduction

An osmotic membrane bioreactor (OMBR) that integrates an activated sludge process with a forward osmosis (FO) membrane was firstly proposed by Cornelissen et al. at 2008 (Cornelissen et al., 2008). In the past decade, OMBR technology has aroused increasing interest in the field of wastewater treatment and reclamation due to the advantages of better product water quality and lower fouling tendency as compared with traditional membrane bioreactors (MBRs) (Nguyen et al., 2015; Wang et al., 2017; Xu et al., 2020). However, there are still bottlenecks in OMBR that hinder its wider application in wastewater treatment and reclamation, e.g., low water flux, salt accumulation, membrane fouling and draw solute recovery (Lee and Hsieh, 2019; Wang et al., 2016a). Draw solute recovery is an essential component in OMBR, by which the draw solute is recycled and the high-quality product water is obtained. Currently, the common approaches for draw solute recovery, including reverse osmosis (RO), nanofiltration (NF) and membrane distillation (MD), consume a large amount of energy to drive the separation process (Eriksson et al., 2005; Luo et al., 2017; Vinardell et al., 2020), directly resulting in a substantial increase in energy consumption and operational cost of OMBR. This is regarded as one of the biggest obstacles on the development and application of OMBR for wastewater treatment and reclamation.

In the operation of FO filtration, there is a natural concentration gradient between the two sides of membrane, i.e., a high concentration draw solution (DS) and a low concentration feed solution (FS). Osmotic energy is generated upon the water passes through semipermeable membrane and mixes with the draw solution in the FO process (R. Pattle, 1954). Recent years, osmotic energy has attracted increasing interest because it is a new clean energy that can be sustainably generated with no constraints of the meteorological and geographical conditions (Einarsson and Wu, 2021; Shi et al., 2021). Pressure retarded osmosis (PRO) is one of the most promising technologies for harnessing osmotic energy (Helfer et al., 2014; Son et al., 2016; Thorsen and Holt, 2009). During PRO operation, the DS is pressurized and fed into membrane module by a high-pressure pump, and the water from FS permeates into the DS side through the membrane against the hydraulic pressure, then the volume-expanded DS is depressurized via a hydro-turbine to convert osmotic energy to electric power. Compared with conventional FO, the PRO process not only demonstrates similar solute rejection performance but also recovers osmotic energy (Patel et al., 2014; Sakai et al., 2016; Wan and Chung, 2015). The obtained energy can be further utilized to compensate for the energy need of water recovery process.

Inspired by osmotic energy recovery in the PRO process, replacing the FO process in OMBR with a PRO process with aim to simultaneously recover osmotic energy and clean water seems to be a potential way to improve the energy efficiency of OMBR. Based on this, present study proposed a novel PRO-MBR of integrating the bioreactor with the PRO process. Existing studies on PRO process mostly employed clean water, river water or low-strength wastewater as FS to evaluate the power generation performance (Kim et al., 2015; O'Toole et al., 2016; Wan and Chung, 2015). The power density of PRO varied significantly with different FS since the concentration and composition of FS closely relate to the water flux and membrane fouling in PRO, which directly or indirectly determines the energy recovery efficiency (Bar-Zeev et al., 2015; She et al., 2017a, 2013; Yip and Elimelech, 2011). To the best of our knowledge, there has been no study focusing on the power generation performance of PRO with sludge mixed liquor as FS. Only one previous paper of ours reported the fouling characteristics in PRO coupled with activated sludge process (Meng et al., 2020). Thus, the power generation performance of PRO-MBR and how much the energy consumption can be reduced as compared with conventional FO-MBR, as well as how the membrane fouling influences the power generation performance in PRO-MBR deserve to be further studied.

To this end, a lab-scale PRO-MBR system was established and a comparative study with conventional FO-MBR was then conducted under AL-DS (active layer facing FS) and AL-FS (active layer facing DS) mode. The contaminants removal performance, water flux, power generation performance, membrane fouling behavior and fouling reversibility were comprehensively investigated for both PRO-MBR and FO-MBR with the aim to assess the potential of the PRO-MBR for wastewater treatment and energy recovery.

2. Materials and methods

2.1 Experimental setup

A laboratory-scale PRO-MBR comprised of a bioreactor and an FO membrane module was established in this study (Fig. S1). The bioreactor with an effective volume of 1.7 L was full of activated sludge (collected from municipal WWTP), and an aeration diffuser was placed at the bottom. The membrane module was constituted by two identical flow channels (85 mm × 50 mm × 1.5 mm) for FS and DS streams, respectively, with membrane coupon mounted between the two channels. A commercial FO membrane made of cellulose triacetate (CTA) (supplied by Hydration Technologies Innovations, Albany, OR) with an effective membrane area of 25.5 cm^2 was used in this study. Both the active layer and the support layer of the FO membrane were filled with a tricot-type spacer (She et al., 2017b). The mixed liquor in the bioreactor was circulated by a peristaltic pump (BT100-2J, Longer Precision Pump, China) through the FS flow channel with a cross-flow velocity of 10.3 cm/s, meanwhile a NaCl solution with a concentration of 2 M (osmotic pressure of 9.9 MPa) was pressurized and circulated by a high-pressure pump (DP-130, Xinxishan, China) through the DS flow channel, with a cross-flow velocity of approximately 177 cm/s. The DS tank was placed on a digital balance (PL6001E， Mettler Toledo, China), and the DS weight change was continuously recorded by a computer. To make a fair comparison, a FO-MBR with the entire system the same expect without applied hydraulic pressure on DS stream was operated in parallel. The DS solution was circulated by another identical peristaltic pump through the DS flow channel with a cross-flow velocity of 10.3 cm/s.

2.2 Operation conditions

During the whole experiment, the PRO-MBR and FO-MBR were operated at temperature of 25 ± 1 °C. The hydraulic retention time (HRT) varied in the range of 32 to 74 h along with the flux variation in the operation of FO, and no sludge was discharged during the experiment. Synthetic domestic wastewater was used as the feed water with chemical oxygen demand (COD), total organic carbon (TOC), total phosphorus (TP), total nitrogen (TN) and NH_4^+-N concentrations of 373.3 ± 17.2 mg/L, 81.96 ± 1.68 mg/L, 2.08 ± 0.13 mg/L, 38.24 ± 1.68 mg/L and 24.88 ± 1.50 mg/L, respectively. The composition of synthetic wastewater was set according to that reported in literature (Wang et al., 2014). The sludge collected from a secondary sedimentation tank at the Taihu Xincheng Wastewater Treatment Plant (Wuxi, China) was employed as the seed sludge. It was cultivated in the same bioreactor with synthetic wastewater for approximately 15 days before starting the operation. The initial sludge concentration in the PRO-MBR and FO-MBR were both 3.0 g/L for mixed liquor suspended solids (MLSS) and 2.1 g/L for mixed liquor volatile suspended solids (MLVSS). The aeration rate was approximately 100 L/h, and the corresponding DO concentration in the bioreactors were maintained in the range of 4-5 mg/L.

Membrane orientation is a critical factor that largely determines the water flux and membrane fouling behavior in FO and PRO processes (Kim et al., 2016). Therefore, both AL-FS orientation and AL-DS orientation were applied in the operation of PRO-MBR and FO-MBR. As for PRO-MBR, the additional hydraulic pressure applied on the DS side was set as 6 bar (0.6 MPa), which ensured that the FO membrane was maintained mechanically stable in both orientations. The pristine FO membrane was first preconditioned for 4 h in the membrane module in advance to obtain its stable initial water flux (She et al., 2017a).

In addition, at the end of each experiment, the fouled membrane was *in situ* physically cleaned for 1 h using 0.08 M NaCl as the FS and deionized water as the DS (i.e., osmotic backwash), according to the method reported in previous literature (Yuan et al., 2015). The DI water flux was retested for the membranes after cleaning and compared with that of pristine membrane, based on which the fouling reversibility was then assessed.

2.2 Analytical methods

The contaminants concentrations in the permeate, mixed liquor supernatant and feed water were periodically measured for both PRO-MBR and FO-MBR. The concentrations of NH_4^+-N, PO_4^{3-}-P, TN, TO, MLSS and MLVSS were determined according to the standard method (APHA, 1998), and the TOC concentration was analyzed by a TOC analyzer (TOC-Vcsh, Shimadzu, Japan).

The water flux (J_w) was calculated via the variation of DS weight (according to Eq. (1)), which was continuously recorded by a digital balance connected to a computer.

$$J_w = \frac{\Delta V}{A \times \Delta t} \qquad (1)$$

where ΔV (L) is the collected permeate volume over a pre-determined duration Δt (h), A is the active membrane area (m^2). To eliminate the impacts of the initial water flux of different FO membranes, the normalized flux was used to characterize the water flux performance during the operation of PRO-MBR and FO-MBR. The water flux was normalized by Eq. (2).

$$J' = \frac{J_w}{J_0} \qquad (2)$$

where J' is the normalized flux, J_0 is the initial water flux of the FO membrane (L/ (m^2

h)). In addition, the water fluxes after fouling and after physical cleaning were measured to evaluate the flux recoverability in PRO-MBR and FO-MBR. The flux recovery rate was calculated by Eq. (3).

$$R = \frac{J_2 - J_1}{J_0 - J_1} \qquad (3)$$

where R is the flux recovery rate (%), J_1 is the water flux of the fouled FO membrane before physical cleaning (L/(m^2 h)), and J_2 is the water flux of the fouled FO membrane after physical cleaning (L/(m^2 h)).

Power density is widely used to assess the power generation performance of PRO. It is defined as the osmotic energy output per unit membrane area (Han et al., 2016b) and it can be calculated by Eq. (4).

$$W = \frac{J_w \times \Delta P}{36} \qquad (4)$$

where W is the power density (W/m^2), J_w is the water flux of the FO membrane (L/ (m^2 h)), and ΔP is the effective hydraulic pressure difference across the membrane (bar).

Specific energy consumption (SEC) was usually used to evaluate the energy efficiency of water recovery process (Seo et al., 2019). SEC is defined as the energy consumed for generating one unit volume of product water and it can be calculated for PRO and FO by Eq. (5).

$$SEC = SEC_{pumping} + SEC_{DS\ regeneration} - SEG \qquad (5)$$

where $SEC_{pumping}$ is the energy consumption of pumping FS/DS, $SEC_{DS\ regeneration}$ is the energy consumption of DS generation process, specific energy generation (SEG) is the energy generated by PRO while unit volume of product water is generated. The $SEC_{pumping}$ of pump was calculated by Eq. (6). and the W_{pump} of high-pressure pump (for pressurizing DS) with energy recovery device was calculated by Eq. (7) (Kim et al., 2013).

$$SEC_{pumping} = \frac{W_{pump} \times 24h}{V_{product\ water}} \qquad (6)$$

$$W_{pump} = \Delta P \times Q_{DS} \times (1 - \eta_{ERD}) \qquad (7)$$

where W_{pump} is the pump power, Q_{DS} is the DS flow rate, η_{ERD} is the efficiency of energy recovery device (95% in present study), $V_{product\ water}$ is the product water volume per day (m^3). RO is the normally employed way for DS regeneration in FO, thus $SEC_{DS\ regeneration}$ is calculated based on the RO as DS regeneration process in present study. The software ROSA 9.1 (Dow Filmtec) was used to simulate and calculate the SEC of RO for DS generation (to be 1.38 kWh/m^3); Meanwhile, the SEC of RO for DS regeneration (under similar operation conditions) reported in literature was in the range of 1.37-1.5 kWh/m^3 (Chia et al., 2021; Kim et al., 2015; Seo et al., 2019; Zaviska et al., 2015). Therefore, present study takes 1.4 kWh/m^3 for the following calculation in reference of both the simulated value and the reported value. The energy generated by PRO process can be further utilized to reduce the SEC. The SEG can be calculate d as per Eq. (8).

$$SEG = \frac{W \times \eta \times 10^{-3} \times 24h \times A}{V_{product\ water}} \qquad (8)$$

where η is the energy conversion efficiency (95% in present study).

At the end of experiments, the fouled FO membranes were carefully collected for fouling characteristic analyses. A field emission scanning electron microscope (FESEM) (S-4800, Hitachi, Japan) and an energy-dispersive X-ray (EDX) analyzer (Falcon, EDAX Inc., USA) were used to characterize the morphology and chemical composition of the fouled FO membranes. In addition, a confocal laser scanning microscope (CLSM,

LSM 710, ZESIS, Germany) was applied to characterize the distributions of organic foulants and biofoulants on the fouled FO membrane surfaces and within porous support layer. The target foulants, including α-D-glucopyranose and β-D-glucopyranose polysaccharides, proteins and microorganisms, were stained by concanavalin A (ConA), calcofluor white (CW), fluorescein isothiocyanate (FITC) and SYTO 63, respectively, before characterization. Details of the specific methods of the SEM, EDX and CLSM analyses can be found in our previous publications (Wang et al., 2016b; Yuan et al., 2015).

3. Results and discussion

3.1 Contaminants removal performance

Firstly, contaminants removal performance of PRO-MBR and FO-MBR were investigated and compared. The two identical MBRs were operated in parallel for more than 30 days to achieve stable biological treatment performance before the start-up of PRO-MBR and FO-MBR. Table 1 summarizes the concentrations of TOC, NH_4^+-N, TN and TP in the influent, supernatant and permeate, as well as their corresponding removal rates in PRO-MBR and FO-MBR.

Excellent removal performances of organic matters and nutrients were achieved in both PRO-MBR and FO-MBR regardless of the membrane orientation. The TOC removal rate and NH_4^+-N removal rate were > 96% and > 98%, respectively, for both PRO-MBR and FO-MBR; moreover, no TOC and NH_4^+-N accumulation was observed in the supernatant, thus this result should be mainly attributed to the biodegradation of microorganisms in the bioreactor. In addition, effective removal of TN (> 96%) and TP (approximately 100%) were also achieved in both PRO-MBR and FO-MBR. Considering the dominating aerobic condition in the MBRs, such high removal performance of TN and TP should be mainly attributed to the high rejection ability of FO membrane to nitrite, nitrate and phosphate. As a result, high-quality product water, with TOC < 3 mg/L, NH_4^+-N < 1 mg/L, TN < 1 mg/L and TP not detected, were achieved in both PRO-MBR and FO-MBR. Overall, the contaminants removal performance of the PRO-MBR was comparable with that of FO-MBR, and consistent with previous reports on the osmotic MBRs for treating municipal wastewater (Qiu et al., 2016; Vinardell et al., 2021). PRO-MBR (same as FO-MBR) combines the biodegradation and bioconversion effects of bioreactor with the high retention effect of FO membrane, by which high-efficiency pollutants removal was achieved and high-quality water recovery can be guaranteed.

It is noteworthy that in a typical PRO process with wastewater as FS, the contaminants cannot be removed but be retained and accumulated in the FS side. Hence, management of the concentrate should be carefully considered. However, there was no TOC and NH_4^+-N accumulation phenomenon in the FS during the operation of PRO-MBR, as suggested by the contaminant concentrations in the supernatant (shown in Table 1), due to the biodegradation and bioconversion effects of microorganisms in the bioreactor. With regard to TN, it can be readily removed by applying A/O-MBR or employing biofilm system. Therefore, the treatment of PRO concentrate, which could inevitably increase the cost and induce secondary pollutants, can be avoided and the sustainability and technoeconomic of PRO process will be improved. In addition, previous study reported that OMBR exhibited lower fouling propensity compared with direct FO process for municipal wastewater in long-term operation, because much of the potential organic foulants in wastewater was degraded by bacteria in MBR (Sun et al., 2016). Thus, a combination of MBR with PRO should be advantageous to fouling control in PRO. In summary, such a novel PRO-MBR system is potentially able to achieve simultaneous energy and water recovery in a sustainable way.

Table 1
TOC, NH_4^+-N, TN and TP concentrations in the influent, sludge supernatant and FO permeate and their removal rates (average ± standard deviation from triple measurements) in FO-MBR and PRO-MBR.

Contaminants	Concentrations and removal rates	PRO-MBR AL-DS	PRO-MBR AL-FS	FO-MBR AL-DS	FO-MBR AL-FS
TOC	Influent (mg/L)	78.49 ± 4.73	77.49 ± 3.56	78.88 ± 1.57	77.56 ± 2.83
	Sludge supernatant (mg/L)	4.99 ± 2.41	3.50 ± 2.75	3.86 ± 1.15	4.36 ± 0.95
	FO permeate (mg/L)	2.77 ± 1.51	2.07 ± 1.45	2.86 ± 0.76	2.74 ± 0.10
	Removal rate (%)	96.47 ± 1.10	97.33 ± 1.12	96.37 ± 0.51	96.46 ± 0.10
NH_4^+-N	Influent (mg/L)	25.06 ± 1.64	25.43 ± 0.89	24.86 ±0.75	25.34 ± 0.75
	Sludge supernatant (mg/L)	0.28 ± 0.21	0.46 ± 0.28	0.34 ± 0.12	0.51 ± 0.19
	FO permeate (mg/L)	0.37 ± 0.07	0.32 ± 0.03	0.26± 0.05	0.39± 0.04
	Removal rate (%)	98.52 ± 1.18	98.74 ± 0.26	98.95± 0.69	98.46± 0.62
TN	Influent (mg/L)	28.73 ± 2.34	28.36 ± 1.85	29.64 ± 1.95	28.49 ± 2.18
	Sludge supernatant (mg/L)	30.58 ± 2.17	30.47 ± 1.24	31.24 ± 1.55	29.98 ±1.87
	FO permeate (mg/L)	0.78 ± 0.06	0.89 ± 0.05	0.85 ± 0.08	0.61 ± 0.09
	Removal rate (%)	97.29 ± 1.28	96.86 ± 0.39	97.13 ± 0.90	97.86 ± 0.68
TP	Influent (mg/L)	1.95 ± 0.05	2.08 ± 0.04	2.06 ± 0.01	2.12 ± 0.03
	Sludge supernatant (mg/L)	0.28 ± 0.20	0.34 ± 0.18	0.12± 0.09	0.36 ± 0.13
	FO permeate (mg/L)	ND	ND	ND	ND
	Removal rate (%)	100	100	100	100

3.2 Water flux performance

The water flux profiles of PRO-MBR and FO-MBR with different membrane orientations are shown in Figure 1a and Figure 1b, respectively. Generally, water flux in the FO-MBR was slightly higher (stable flux of 12.1 and 10.8 LMH for AL-DS and AL-FS, respectively) than in PRO-MBR (stable flux of 11.3 and 8.5 LMH for AL-DS and AL-FS, respectively) in both two membrane orientations. In PRO system, the draw solution is pressurized in order to convert the osmotic power to mechanical energy (Shi et al., 2021). This additional hydraulic pressure reduces the permeation driving force (osmotic pressure difference) across the membrane thus inducing water flux decline. In present study, a hydraulic pressure of 0.6 MPa was applied on DS side which was much lower than the osmotic pressure deference across membrane (approximately 9.0 MPa) with 2 M NaCl as DS and domestic wastewater as FS. Therefore, PRO-MBR can achieve comparable water flux with that in conventional FO-MBR.

Membrane orientation is a critical operational parameter for FO and PRO processes, which substantially influences the water flux performance, the fouling propensity and the membrane stability. The water flux performances of PRO-MBR in AL-DS and AL-FS orientation were compared, consequently. In general, the water flux of membrane operated in AL-DS orientation was consistently higher than that of under AL-FS orientation, i.e., both a higher initial flux (20.0 LMH versus 8.6 LMH) and a higher stable flux (10.6 LMH versus 7.5 LMH) were achieved under the AL-DS orientation. Similar result was also obtained in FO-MBR. The better water flux performance under AL-DS orientation, which was expectable in FO, can be attributed to the less severe internal concentration polarization (ICP) effect under AL-DS orientation than that under AL-FS orientation (McCutcheon and Elimelech, 2006; Tang et al., 2010). As for PRO operated in AL-FS orientation, with the porous and thick support layer facing DS, the mixing of high concentration DS and permeate from FS was retarded in support layer, thus resulting in the dilution of DS at the interface of active layer and support layer, and consequently the reduction of osmotic pressure difference across the membrane (permeation driving force). While in AL-DS orientation, with support layer facing FS, the concentrative ICP effect in support layer is relatively lower because the low concentration of FS, thus the influence on osmotic pressure difference is much lower than that in AL-FS orientation. The higher the water flux is, the higher the power density can be achieved in PRO process, therefore the AL-DS orientation is normally adopted for PRO.

In contrast, the FO-MBR is normally operated under AL-FS orientation to avoid serious membrane fouling in the support layer of the FO membrane (Honda et al., 2015). Indeed, as shown in Figure 1, the water flux decline in AL-DS orientation was more significant than that in AL-FS orientation for both FO-MBR and PRO-MBR, though the initial flux in AL-DS orientation was much higher. The water flux profiles of membrane operated in AL-DS orientation exhibited typical 2-stage decline curve for both FO-MBR and PRO-MBR, i.e., the water flux in AL-DS orientation dropped rapidly in the first 50 minutes and then stabilized, however, the water flux maintained a relatively stable level in AL-FS orientation during the whole operation period. In AL-DS orientation, where the porous support layer facing mixed liquor, the pollutants can be easily carried into and adsorbed within support layer, moreover the activated sludge also can be directly deposit on support layer surface, which collectively caused rapid flux decline at the beginning of operation; and once a stable cake layer was formed on support layer surface, the penetration of pollutants into support layer might be slowed down due to barrier effect of cake layer, therefore the flux variation proceeded to a gradual decline phase. This result implied that membrane fouling behavior was highly dependent on the membrane orientations in PRO-MBR. Considering the power generation efficiency, PRO is normally operated in AL-DS orientation, however the fouling propensity need to be seriously considered for PRO-MBR in which sludge mixed liquor is used as FS (facing the support layer of membrane).

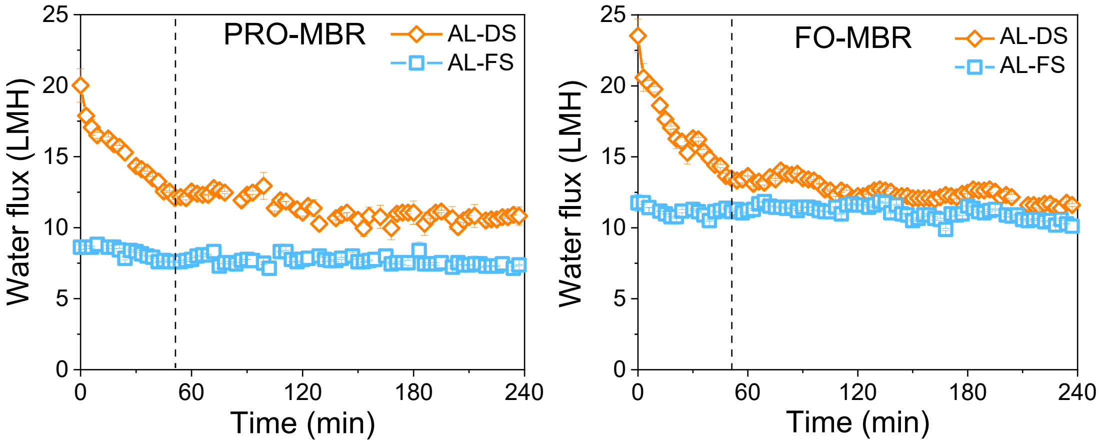

Figure 1 Water flux profiles in PRO-MBR and FO-MBR with different membrane orientations (i.e., AL-DS and AL-FS)

3.3 Power generation performance

Previous studies demonstrated that substantially different power generation performances were obtained in PRO process in different membrane orientations (AL-FS and AL-DS). Though PRO was normally recommended to operate in AL-DS orientation considering the higher power density and better membrane stability, there is still controversy on which orientation is better when wastewater (with high fouling potential) is used as FS. In AL-DS orientation, membrane is more prone to fouling with porous support layer facing wastewater, as a consequence, the advantage of high power density and technoeconomic will be compromised.

This study, for the first time, investigated the power generation performances of PRO-MBR (with sludge mixed liquor as FS) operated in AL-DS and AL-FS orientation. Figure 2 presents the power density curves of PRO-MBR in AL-DS and AL-FS orientation. The power density profiles of PRO-MBR (for both two orientations) were observed to follow the similar variation trend of membrane fluxes (as shown in Fig. 1). Based on the fact that the power density is directly proportional to the water flux (according to Eq. (4)), PRO-MBR operated in AL-DS orientation (with a better flux performance than in AL-FS orientation) undoubtedly achieved a higher power density, i.e., the power density ranged from 3.4-1.8 W/m^2 in the AL-DS orientation while it was only around 1.4 W/m^2 in the AL-FS orientation. Likewise, this can be simply explained by the fact that the dilutive ICP in AL-FS mode was more severe than the concentrative ICP in AL-DS mode, thus leading to lower flux and poorer power density.

It was reported that with the same membrane orientation of AL-DS, similar DS concentration (2 M NaCl) and applied pressure (6.0-6.5 bar) on the DS side, the peak power density of the PRO process was normally around 4.0 W/m^2 (Kim et al., 2016; She et al., 2013, 2012b). On the other hand, it was reported that the power density of a PRO process was largely compromised due to membrane fouling when real wastewater was used as the feed (Wan and Chung, 2015). Thus, considering the high concentration and complexity of sludge mixed liquor as FS, it is reasonable that the maximum power density achieved in PRO-MBR (3.4 W/m^2 in AL-DS orientation) was lower than that in ideal condition.

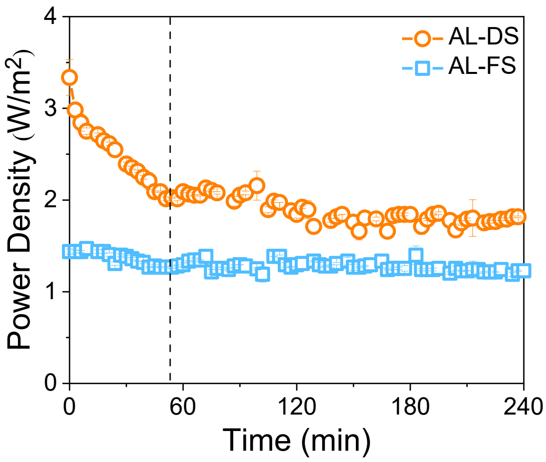

Figure 2 Power density profiles of PRO-MBR operated in different membrane orientations (i.e., AL-DS and AL-FS).

3.4 Techno-economic analysis

To evaluate how much energy consumption can be reduced by replacing FO with PRO in a OMBR system, the specific energy consumption (SEC) of FO and PRO under AL-DS orientation were analyzed and compared (as shown in Table 2). Energy consumption of a conventional FO system was basically comprised of two aspects: the pumping for FS and DS and the RO process for DS regeneration. As shown in Table 2, the SEC of conventional FO system was 1.427 kWh/m^3, in which RO for DS regeneration was the dominant energy consuming component (1.4 kWh/m^3). This accounted for 98.2% of the total energy consumption. In contrast, besides the equal energy consumption of RO for DS regeneration, additional hydraulic pressure was applied on DS side in the PRO process, thus the energy consumption was relatively higher (1.451 kWh/m^3) than that of conventional FO process.

However, osmotic energy was harvested during the PRO process, then the osmotic energy can be further converted to electricity energy as energy supplement by a turbo device. In present study, 0.168 kWh energy was generated along with per m^3 water production by PRO process. Considering this additional energy supplement, the net specific energy consumption of the PRO process eventually came to 1.297 kWh/m^3, a reduction of 10.09% was achieved via replacing FO with PRO in a OMBR system with otherwise conditions identical. Overall, with the ability of recovering osmotic energy while wastewater treatment, the PRO-MBR showed better economicalness than conventional FO-MBR in the fields of wastewater treatment and reclamation.

It is noteworthy that membrane fouling is a critical factor affecting the power generation performance in PRO-MBR. As shown in Figure 2, PRO exhibited the maximum power density (as high as 3.4 W/m^2) at the very beginning of operation, however it declined rapidly as the operation proceeded and stabilized at 1.8 W/m^2. Correspondingly, the energy generation performance decreased from 0.317 kWh/m^3 to 0.168 kWh/m^3 (a reduction of 47.05%). This can be attributed to the formation of fouling layer on support layer of FO membrane during the initial filtration (as discussed in Section 3.2). If such membrane fouling can be mitigated (e.g., applying bio-carriers, quorum quenching strategy, fabricating FO membrane with low S value, etc.), the power density and technoeconomic competitiveness of PRO-MBR could be largely improved. Furthermore, in present study, a relatively low applied hydraulic pressure (6 bar) was employed in PRO with the aim to prevent membrane deformation under long-term operation. The applied hydraulic pressure is lower than the theoretical optimum (around 45 bar for present study) for power generation. Therefore, fabricating FO membrane with high mechanical strength (able to withstand high hydraulic pressure) could be another approach to improve the power generation performance of PRO-MBR.

In summary, the results of present study preliminarily demonstrated the good techno-economic potential of the PRO-MBR, while there is still a big room for improvement.

Table 2

The specific energy consumption of FO and PRO

	FS/DS feeding pump [a] (kWh/m^3)	High-pressure pump on DS [b] (kWh/m^3)	RO for DS regeneration [c] (kWh/m^3)	Specific Energy generation [d] (kWh/m^3)	Specific energy consumption (kWh/m^3)
FO	0.027	-	1.4	-	1.427
PRO	0.011	0.040	1.4	0.168	1.283

[a] The feeding pump energy consumption was calculated as: $W_{pump} \times 24$ h / $V_{water\ production}$.

[b] The energy consumption of high-pressure pump with energy recovery device was calculated as: $\Delta P \times Q_{DS} \times (1-\eta_{ERD}) \times 24h / V_{water\ production}$.

[c] Energy consumption of RO for DS regeneration was calculated to be 1.38 kWh/m^3 by ROSA 9.1 (Dow Filmtec) was; moreover, the SEC of RO for DS regeneration reported in literature was in the range of 1.37-1.5 kWh/m^3 (Chia et al., 2021; Kim et al., 2015; Seo et al., 2019; Zaviska et al., 2015); present study takes 1.4 kWh/m^3 for the following calculation in reference of both the simulated value and the reported values.

[d] The specific energy generation of PRO was calculated as: $W_{PRO} \times \eta_{PRO} \times 10^{-3} \times 24h \times A / V_{water\ production}$.

W_{pump} and $V_{water\ production}$ refer to pump power and water production per day; ΔP, Q_{DS}, η_{ERD} refer to applied pressure on DS, DS flow rate and energy recovery efficiency, respectively; W_{PRO}, η_{PRO} and A refer to power density of PRO, energy conversion efficiency of PRO and the effective membrane area, respectively.

3.5 Membrane fouling characteristics

It was showed in previous section that the power density in PRO-MBR was highly influenced by membrane fouling. Understanding the fouling characteristics in PRO-MBR is quite essential for developing effective fouling control strategy, and thereby further improving the power density and sustainability of PRO-MBR.

Because of the fact that hydraulic conditions in PRO-MBR was different with that in FO-MBR, the fouling characteristics in PRO-MBR would be distinct from that in FO-MBR as well. In addition, unlike the AL-FS membrane orientation that is normally adopted in FO, PRO process is usually operated in AL-DS mode (porous support layer facing FS) to achieve higher power density. Therefore, in the case of sludge mixed liquor as FS, the fouling process could be even more complex in PRO-MBR. With the aim to clarify the fouling characteristics in PRO-MBR, the fouled membranes of FO-MBR and PRO-MBR (in both AL-DS and AL-FS orientations) were collected at the end of experiments and characterized by SEM, EDS and CLSM.

Figure 3 presents the SEM images of the side of membranes facing FS (sludge mixed liquor). It is obvious that a sludge cake layer had formed on membranes in AL-DS orientation (support layer facing FS) for both FO-MBR and PRO-MBR, while the fouling on membranes in AL-FS orientation (active layer facing FS) was negligible. Compared to the dense and smooth active layer, the support layer with porous and thick structure was very prone to fouling. It was reported that in the PRO process treating municipal wastewater, most of the fouling occurred in the pores of the support layer (Han et al., 2016a; She et al., 2017b). However, the observed significant sludge cake layer on support layer of membranes in present study indicated that with activated sludge mixed liquor as FS (in AL-DS orientation), the fouling was not only distributed within the pores of support layer but also deposited on the surface of support layer.

The element composition of the fouling layers on membranes were further analyzed by EDS. As shown in Figure 3, C, N, O, Na, Cl, P and S were the major elements on membranes fouled in AL-DS orientation for both PRO-MBR and FO-MBR. The presence of Na and Cl on fouled membrane surfaces was the result of reverse salt transport from DS side (Luján-facundo et al., 2017). Additionally, since the pristine CTA-FO membrane only contains C and O, the abundant N element and considerable P and S content suggested that organic fouling or biofouling was formed on membrane surfaces, which was consistent with the finding of sludge cake layer via SEM images. Furthermore, Ca element was also observed on membrane fouled in AL-DS orientation, though with a low intensity, which suggested inorganic ions was involved in the membrane fouling (via complexation or scaling effects). In contrast, the Ca and P element were undetected on the membranes fouled in AL-FS orientation for both PRO-MBR and FO-MBR, moreover, the peak intensities of other elements were generally lower than those on membranes fouled in AL-DS orientation. This result further confirmed that membrane fouling in AL-DS orientation was more severe and complex.

Considering the complexity of membrane fouling in the AL-DS orientation (porous support layer facing mixed liquor), the cross-section of the membranes fouled in the AL-DS orientation was further investigated by SEM-EDS. As shown in Figure 2S, fouling took place as expected within the porous support layer of membranes in both FO-MBR and PRO-MBR. It is noteworthy that unlike the fouling layer on the surface of support layer, intensive accumulation of Ca and P within support layer of membranes was observed from the EDS mapping images, implying that inorganic scaling as a result of the precipitation of Ca and P ions probably took place within support layer (She et al., 2017a).

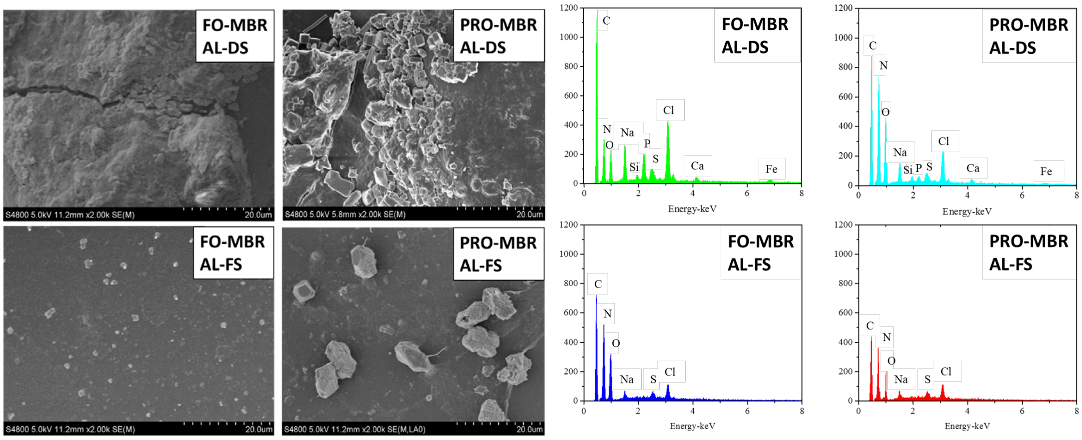

Figure 3 SEM images (left) and EDS spectra (right) of the fouled FO membranes in the PRO-MBR and FO-MBR.

Biofouling is normally regarded as the dominant fouling type in membrane bioreactor. To achieve a deeper understanding of the biofouling characteristics in PRO-MBR, the distributions and the contents of bio-foulants (e.g., polysaccharides, proteins and microorganisms) on fouled membranes were further analyzed by CLSM coupled with multiple fluorescence labeling (Li et al., 2019; Wang et al., 2016b; Yuan et al., 2015). As shown in Figure 4, the surface of membranes fouled in AL-DS orientation (for both PRO-MBR and FO-MBR) were covered with thick biofouling layers (both around 60 μm thick); Since the support layer of FO membrane was approximately 30 μm thick, it can be inferred that the foulants were indeed located not only within the pores but also on the surface of the support layer. By contrast, the biofouling layers on membranes fouled in the AL-FS orientation were much thinner (approximately 20 μm thick), and the foulants were all deposited on the surface of the active layer. This finding was in consistence with above observations of the fouled FO membranes via SEM and EDX, that membrane fouling was more severe and complex in the AL-DS orientation.

A quantitative analysis was further conducted on the fouling layers. The biovolume of various bio-foulants in fouled membrane was calculated by *PHLIP* software (Yuan et al., 2015) and the results are summarized in Table 3. The total biovolume of polysaccharides, proteins and microorganisms on membranes fouled in AL-DS orientation were 30.98 $\mu m^3/\mu m^2$ and 16.92 $\mu m^3/\mu m^2$ for FO-MBR and PRO-MBR, respectively, which were much higher than those in membrane fouled in AL-FS orientation, i.e., 3.29 $\mu m^3/\mu m^2$ in PRO-MBR and 4.84 $\mu m^3/\mu m^2$ in FO-MBR. This result further demonstrated that biofouling on membranes fouled in AL-DS orientation was much more significant.

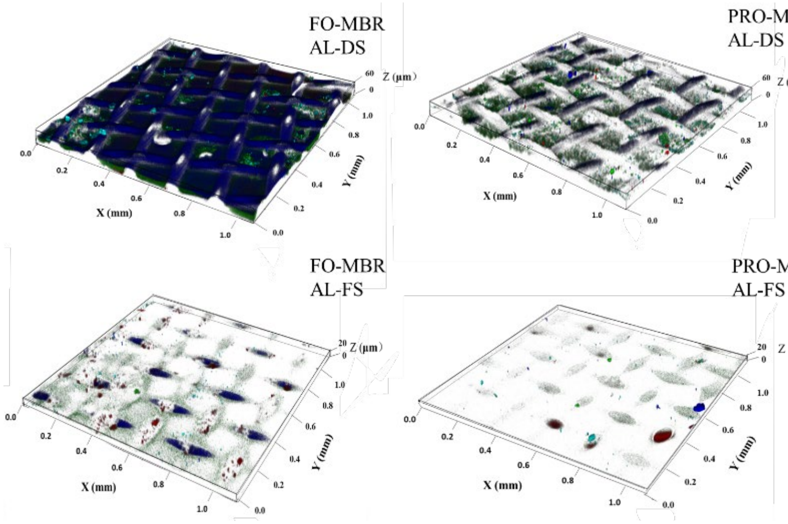

Figure 4 CLSM images of the fouled FO membranes in different membrane orientations in the PRO-MBR and FO-MBR (the cyan, blue, green and red colors represent α-D-glucopyranose, β-D-glucopyranose, proteins, and microbial cells, respectively).

Table 3

Biovolume of the foulants on the fouled FO membranes in PRO-MBR and FO-MBR (calculated by PHLIP). [a]

		α-D-glucopyranose ($\mu m^3/\mu m^2$)	β-D-glucopyranose ($\mu m^3/\mu m^2$)	Proteins ($\mu m^3/\mu m^2$)	Total cells ($\mu m^3/\mu m^2$)	Sum ($\mu m^3/\mu m^2$)
PRO-MBR	AL-DS	0.21 ± 0.07	7.13 ± 0.71	6.51 ± 0.33	3.07 ± 0.66	16.92 ± 1.77
	AL-FS	0.88 ± 0.14	0.63 ± 0.06	1.06 ± 0.21	0.72 ± 0.08	3.29 ± 0.49
FO-MBR	AL-DS	2.01 ± 0.64	11.13 ± 1.03	9.99 ± 0.42	7.85 ± 0.78	30.98 ± 1.87
	AL-FS	2.00 ± 0.09	1.07 ± 0.04	1.37 ± 0.08	0.40 ± 0.03	4.84 ± 0.24

[a] Values are given as the mean values ± standard deviation (number of measurements: n = 3).

Above results collectively indicated that membrane orientation largely determined the fouling behavior in PRO-MBR and FO-MBR. The PRO-MBR, in which membrane was normally operated in AL-DS orientation, suffered more severe and complex membrane fouling, as compared with FO-MBR (membrane normally operated in AL-FS orientation). From another point of view, AL-FS orientation could be a more promising option in the scenario of PRO-MBR if the shortcomings of severe ICP and membrane stability (leading to poor power density and membrane damage) can be well addressed.

Additionally, it is interesting to observe that the biofouling in PRO-MBR was obviously less than those in FO-MBR when they were both operated in AL-DS orientation (as shown in Figure 4). The biovolume of polysaccharides, proteins and microorganisms on membranes fouled in PRO-MBR (in AL-DS orientation) were 7.33 ± 1.77, 6.51 ± 0.33 and 3.07 ± 0.66 $\mu m^3/\mu m^2$, respectively, which were all lower than those in FO-MBR (polysaccharides of 13.14 ± 1.69 $\mu m^3/\mu m^2$, proteins of 9.99 ± 0.42 $\mu m^3/\mu m^2$ and microorganisms of 7.85 ± 0.78 $\mu m^3/\mu m^2$). In total, the biofoulants on membrane fouled in PRO-MBR was 45% (in volume) less than those in FO-MBR. Such reduction of biofouling in support layer of membrane in PRO-MBR could be attributed to the result of reverse salt transport. Due to the applied additional hydraulic pressure on DS side, the reverse salt transport was enhanced, thus more salts passed through the active layer, and accumulated in support layer because of the ICP effect. The high salinity stress induced strong inhibitory effect on bioactivity, hence the biofouling was largely restrained. Previous studies generally believed that reverse solute diffusion will enhance the organic fouling in PRO process because the divalent ions (e.g. Ca^{2+}) from DS can promote aggregation of alginate and induce severe pore clogging and cake layer formation (She et al., 2013, 2012a). However, local salinity stress in support layer induced by RSD and its inhibitory effect on the biofouling were not considered in previous studies. Our study provided a new understanding to the effect of RSD on membrane fouling in PRO process.

3.6 Fouling reversibility

Fouling reversibility is an important factor that determines the sustainability and technoeconomic of MBR system (Song et al., 2018, 2017). At the end of experiment, the fouled membranes in PRO-MBR and FO-MBR were physically cleaned and the fouling reversibility was then evaluated.

Figure 5 shows the normalized fluxes of the fouled membranes in PRO-MBR and FO-MBR before and after physical cleaning. Generally, the flux loss of membranes fouled in AL-FS orientation was significantly larger than that in AL-DS orientation for both PRO-MBR and FO-MBR. The normalized flux of membrane after fouling was only 0.51 for PRO-MBR in AL-DS orientation, which was much lower than those for FO-MBR and PRO-MBR in AL-FS orientation (0.85 and 0.86, respectively). This result was in agreement with the result of previous sections that membrane fouling was more severe in AL-DS orientation. In AL-DS orientation, the porous and thick support layer of FO membrane faced the sludge mixed liquor, complex foulants in sludge mixed liquor was easily deposited within the pores, and the aeration scouring effect at membrane surface was unable to completely remove the foulants in support layer, thus leading to inevitable flux decline.

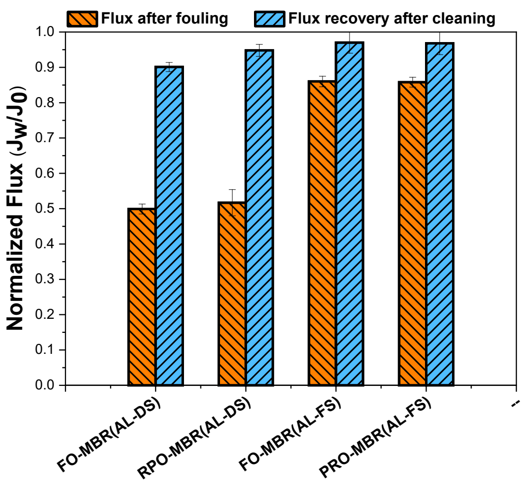

Figure 5 Normalized fluxes of the fouled FO membranes in the PRO-MBR and FO-MBR before and after physical cleaning.

After osmotic backwash of 3 h, the membrane flux was almost completely recovered (both above 95%) for membranes operated in AL-FS orientation for both PRO-MBR and FO-MBR, which indicted that fouling formed in AL-FS orientation (on active layer surface) was mostly reversible. As for membranes oriented in AL-DS orientation, a comparable flux recovery rate of 92.4% was also achieved by physical cleaning for PRO-MBR, suggesting that most of the fouling in support layer was reversible too. Previous study reported that the membrane fouling in FO-MBR (in AL-FS orientation) normally presented high reversibility, the flux recovery rate of 98% was easily achieved by just osmotic backwash (Yuan et al., 2015). This should be mainly attributed to the very low hydraulic pressure applied in FO process. Unlike that in RO and NF processes (driven by high hydraulic pressure), the FO process was driven by osmosic pressure (exclusively on water molecules) difference across the semipermeable membrane, thus the force driving foulants to membrane is much weaker.

Nevertheless, the severe flux loss during operation of PRO-MBR in AL-DS orientation, though mostly reversible, signifies the requirement of high cleaning frequency and operational cost. Additionally, power density is directly proportional to the membrane flux in PRO process, thus the decline of flux also means decrease of power generation performance. Hence, flux decline due to membrane fouling is a critical restricting factor to the performance of RPO-MBR. In view of this, operating PRO-MBR in AL-FS orientation seems a potential way to alleviate membrane fouling, however, as mentioned previously, the severe ICP and membrane stability need to be addressed before.

3.7 Implications

Comparative analysis (as summarized in Table 4) showed that the PRO-MBR exhibited similar excellent contaminants removal performances to that of FO-MBR for municipal wastewater treatment. Additionally, operating flux comparable with that in FO-MBR was also obtained in PRO-MBR under identical operation conditions. More importantly, with the application of PRO process, a considerable amount of energy can be extracted from the osmosis process (not available in FO-MBR), and be further utilized to reduce system energy consumption. Energy consumption is an important factor that determines the feasibility of osmotic MBR in practical application. In this sense, the PRO-MBR system exhibited better application potential than conventional FO-MBR in the field of wastewater treatment and reclamation.

Membrane fouling was an important hindrance to the performance of PRO-MBR. About 40% of the power density was compromised by membrane fouling in PRO-MBR. The power generation performance of PRO-MBR could be further improved if effective fouling control strategies can be developed, e.g., applying bio-carriers, quorum quenching bacteria or antifouling FO membrane material. Furthermore, given the more complex fouling mechanisms, especially biofouling, in PRO-MBR, future research attention should also focus on clarifying its fouling characteristic.

The choice of membrane orientation is of paramount importance for PRO-MBR. Present study found that the energy generation efficiency achieved in AL-DS orientation (4.1 kWh/100 $m^2\cdot d$) was 28.1% higher than that in AL-FS orientation (3.2

kWh/100 m^2·d) with otherwise conditions identical. The relatively lower energy generation efficiency in AL-FS orientation should be attributed to the more severe ICP in support layer for FO membrane operated in AL-FS orientation, which induced lower operating flux, and lower power density as well. Furthermore, the membrane stability was also a big concern for PRO process in AL-FS orientation. However, the inherent advantage of less prone to fouling makes the AL-FS orientation still a potential option for PRO-MBR, in which the severe fouling problem is a critical factor limiting its power density. Therefore, future study on ICP mitigation strategy in AL-FS orientation and high-strength FO membrane should be very necessary.

Table 4

Performance comparison between the FO-MBR and the PRO-MBR.[a]

		FO-MBR		PRO-MBR	
		AL-DS	AL-FS	AL-DS	AL-FS
Operating flux (LMH)		13.54 ± 2.31	11.09 ± 0.45	12.19 ± 2.08	7.79 ± 0.42
Removal rate (%)	TOC	96.51 ± 0.51	96.66 ± 0.10	96.47 ± 1.10	97.33 ± 2.12
	TP	100	100	100	100
	NH_4^+-N	97.49 ± 0.69	98.68± 0.62	98.52 ± 1.18	98.74 ± 0.26
	TN	96.51 ± 0.90	95.96 ± 0.68	97.29 ± 1.28	96.86 ± 0.39
Flux recovery rate (%)		90.10 ± 1.31	97.04 ± 3.45	94.83 ± 1.71	96.82 ± 3.22
Specific energy consumption[b] (kWh/m^3)		1.427		1.283	1.288
Energy generation efficiency[c] (kWh/100 m^2·d)		-	-	4.1	3.2

[a] Values are given as the mean values ± standard deviation (number of measurements: n = 3).
[b] Energy generated by PRO was also considered.
[c] Energy generation efficiency was defined as the energy generated by unit membrane area per day.

4. Conclusion

A novel PRO-MBR was proposed and compared with conventional FO-MBR in this study. PRO-MBR exhibited comparable contaminants removal and water flux performances as compared with FO-MBR. Additionally, a considerable amount of energy (4.1 kWh/100 m^2·d) was generated in PRO-MBR, by which the SEC for water recovery was reduced by 10.02% as compared with FO-MBR. The performance of

PRO-MBR was largely determined by membrane orientation, peak power density of 3.4 W/m^2 was achieved in AL-DS orientation, while that in AL-FS orientation was only 1.4 W/m^2 (because of the severe ICP). However, PRO-MBR suffered more severe and complex membrane fouling when operated in AL-DS orientation. Flux decline induced by membrane fouling restricted the power generation performance of PRO-MBR, especially in AL-DS orientation, the power density was decreased by 38.2% due to the formation of fouling. Future study on PRO-MBR should focus on the control of severe membrane fouling in AL-DS orientation; Moreover, AL-FS orientation could also become a potential option if severe ICP issue was mitigated.

CRediT authorship contribution statement

Shuyue Liu: Conceptualization, Methodology, Investigation, Data curation, Writing - original draft. **Weilong Song**: Conceptualization, Supervision, Methodology, Data curation, Review & editing, Project administration. **Manli Meng**: Methodology, Investigation, Data curation. **Ming Xie**: Review & editing. **Qianhong She**: Review & editing. **Pin Zhao**: Project administration, Review & editing. **Xinhua Wang**: Conceptualization, Supervision, Funding acquisition.

Acknowledgments

This work was supported by the National Natural Science Foundation of China [grant number 51978312]; the Six Major Talent Peaks of Jiangsu Province [grant number 2018-JNHB-014]; and the Program to Cultivate Middle-aged and Young Science Leaders of Colleges and Universities of Jiangsu Province.

Supporting information

Detailed information on additional figures and foulants extracting method can be found in the Supporting Information

References

APHA, 1998. Standard Methods for the Examination of Water and Wastewater- twentieth ed. Am. Public Heal. Assoc. Washington, D.C. https://doi.org/10.1016/j.cej.2017.02.125

Bar-Zeev, E., Perreault, F., Straub, A.P., Elimelech, M., 2015. Impaired Performance of Pressure-Retarded Osmosis due to Irreversible Biofouling. Environ. Sci. Technol. 49, 13050–13058. https://doi.org/10.1021/acs.est.5b03523

Chia, W.Y., Chia, S.R., Khoo, K.S., Chew, K.W., Show, P.L., 2021. Sustainable membrane technology for resource recovery from wastewater: Forward osmosis and pressure retarded osmosis. J. Water Process Eng. 39, 101758. https://doi.org/10.1016/j.jwpe.2020.101758

Cornelissen, E.R., Harmsen, D., de Korte, K.F., Ruiken, C.J., Qin, J.J., Oo, H., Wessels, L.P., 2008. Membrane fouling and process performance of forward osmosis membranes on activated sludge. J. Memb. Sci. 319, 158–168. https://doi.org/10.1016/j.memsci.2008.03.048

Einarsson, S.J., Wu, B., 2021. Thermal associated pressure-retarded osmosis processes for energy production: A review. Sci. Total Environ. 757, 143731. https://doi.org/10.1016/j.scitotenv.2020.143731

Eriksson, P., Kyburz, M., Pergande, W., 2005. NF membrane characteristics and evaluation for sea water processing applications. Desalination 184, 281–294.

https://doi.org/10.1016/j.desal.2005.04.030
Han, G., Zhou, J., Wan, C., Yang, T., Chung, T., 2016a. Investigations of inorganic and organic fouling behaviors , antifouling and cleaning strategies for pressure retarded osmosis (PRO) membrane using seawater desalination brine and wastewater. Water Res. 103, 264–275. https://doi.org/10.1016/j.watres.2016.07.040
Han, G., Zhou, J., Wan, C., Yang, T., Chung, T.S., 2016b. Investigations of inorganic and organic fouling behaviors, antifouling and cleaning strategies for pressure retarded osmosis (PRO) membrane using seawater desalination brine and wastewater. Water Res. 103, 264–275. https://doi.org/10.1016/j.watres.2016.07.040
Helfer, F., Lemckert, C., Anissimov, Y.G., 2014. Osmotic power with Pressure Retarded Osmosis: Theory, performance and trends - A review. J. Memb. Sci. 453, 337–358. https://doi.org/10.1016/j.memsci.2013.10.053
Honda, R., Rukapan, W., Komura, H., Teraoka, Y., Noguchi, M., Hoek, E.M.V., 2015. Effects of membrane orientation on fouling characteristics of forward osmosis membrane in concentration of microalgae culture. Bioresour. Technol. 197, 429–433. https://doi.org/10.1016/j.biortech.2015.08.096
Kim, D.I., Kim, J., Hong, S., 2016. Changing membrane orientation in pressure retarded osmosis for sustainable power generation with low fouling. Desalination 389, 197–206. https://doi.org/10.1016/j.desal.2016.01.008
Kim, D.I., Kim, J., Shon, H.K., Hong, S., 2015. Pressure retarded osmosis (PRO) for

integrating seawater desalination and wastewater reclamation: Energy consumption and fouling. J. Memb. Sci. 483, 34–41. https://doi.org/10.1016/j.memsci.2015.02.025

Kim, J., Park, M., Snyder, S.A., Kim, J.H., 2013. Reverse osmosis (RO) and pressure retarded osmosis (PRO) hybrid processes: Model-based scenario study. Desalination 322, 121–130. https://doi.org/10.1016/j.desal.2013.05.010

Lee, D.J., Hsieh, M.H., 2019. Forward osmosis membrane processes for wastewater bioremediation: Research needs. Bioresour. Technol. 290, 121795. https://doi.org/10.1016/j.biortech.2019.121795

Li, L., Wang, X., Xie, M., Wang, Z., Li, X., Ren, Y., 2019. In situ extracting organic-bound calcium: A novel approach to mitigating organic fouling in forward osmosis treating wastewater via gradient diffusion thin-films. Water Res. 156, 102–109. https://doi.org/10.1016/j.watres.2019.03.018

Luján-facundo, M.J., Soler-cabezas, J.L., Mendoza-roca, J.A., Vincent-vela, M.C., Bes-piá, A., 2017. A study of the osmotic membrane bioreactor process using a sodium chloride solution and an industrial effluent as draw solutions. Chem. Eng. J. 322, 603–610. https://doi.org/10.1016/j.cej.2017.04.062

Luo, W., Phan, H. V., Li, G., Hai, F.I., Price, W.E., Elimelech, M., Nghiem, L.D., 2017. An Osmotic Membrane Bioreactor-Membrane Distillation System for Simultaneous Wastewater Reuse and Seawater Desalination: Performance and Implications. Environ. Sci. Technol. 51, 14311–14320. https://doi.org/10.1021/acs.est.7b02567

McCutcheon, J.R., Elimelech, M., 2006. Influence of concentrative and dilutive internal concentration polarization on flux behavior in forward osmosis. J. Memb. Sci. 284, 237–247. https://doi.org/10.1016/j.memsci.2006.07.049

Meng, M., Liu, S., Wang, X., 2020. Pressure retarded osmosis coupled with activated sludge process for wastewater treatment: Performance and fouling behaviors. Bioresour. Technol. 307, 123224. https://doi.org/10.1016/j.biortech.2020.123224

Nguyen, N.C., Chen, S.S., Nguyen, H.T., Ngo, H.H., Guo, W., Hao, C.W., Lin, P.H., 2015. Applicability of a novel osmotic membrane bioreactor using a specific draw solution in wastewater treatment. Sci. Total Environ. 518–519, 586–594. https://doi.org/10.1016/j.scitotenv.2015.03.011

O'Toole, G., Jones, L., Coutinho, C., Hayes, C., Napoles, M., Achilli, A., 2016. River-to-sea pressure retarded osmosis: Resource utilization in a full-scale facility. Desalination 389, 39–51. https://doi.org/10.1016/j.desal.2016.01.012

Patel, R., Chi, W.S., Ahn, S.H., Park, C.H., Lee, H.K., Kim, J.H., 2014. Synthesis of poly(vinyl chloride)-g-poly(3-sulfopropyl methacrylate) graft copolymers and their use in pressure retarded osmosis (PRO) membranes. Chem. Eng. J. 247, 1–8. https://doi.org/10.1016/j.cej.2014.02.106

Qiu, G., Zhang, S., Srinivasa Raghavan, D.S., Das, S., Ting, Y.P., 2016. Towards high through-put biological treatment of municipal wastewater and enhanced phosphorus recovery using a hybrid microfiltration-forward osmosis membrane bioreactor with hydraulic retention time in sub-hour level. Bioresour. Technol. 219, 298–310. https://doi.org/10.1016/j.biortech.2016.07.126

R. Pattle, 1954. Production of Electric Power by mixing Fresh and Salt Water in the Hydro-electric Pile. Nature 174, 660.

Sakai, H., Ueyama, T., Irie, M., Matsuyama, K., Tanioka, A., Saito, K., Kumano, A., 2016. Energy recovery by PRO in sea water desalination plant. Desalination 389, 52–57. https://doi.org/10.1016/j.desal.2016.01.025

Seo, J., Kim, Y.M., Chae, S.H., Lim, S.J., Park, H., Kim, J.H., 2019. An optimization strategy for a forward osmosis-reverse osmosis hybrid process for wastewater reuse and seawater desalination: A modeling study. Desalination 463, 40–49. https://doi.org/10.1016/j.desal.2019.03.012

She, Q., Jin, X., Li, Q., Tang, C.Y., 2012a. Relating reverse and forward solute diffusion to membrane fouling in osmotically driven membrane processes. Water Res. 46, 2478–2486. https://doi.org/10.1016/j.watres.2012.02.024

She, Q., Jin, X., Tang, C.Y., 2012b. Osmotic power production from salinity gradient resource by pressure retarded osmosis: Effects of operating conditions and reverse solute diffusion. J. Memb. Sci. 401–402, 262–273. https://doi.org/10.1016/j.memsci.2012.02.014

She, Q., Wong, Y.K.W., Zhao, S., Tang, C.Y., 2013. Organic fouling in pressure retarded osmosis: Experiments, mechanisms and implications. J. Memb. Sci. 428, 181–189. https://doi.org/10.1016/j.memsci.2012.10.045

She, Q., Zhang, L., Wang, R., Krantz, W.B., Fane, A.G., 2017a. Pressure-retarded osmosis with wastewater concentrate feed: Fouling process considerations. J. Memb. Sci. 542, 233–244. https://doi.org/10.1016/j.memsci.2017.08.022

She, Q., Zhang, L., Wang, R., Krantz, W.B., Fane, A.G., 2017b. Pressure-retarded osmosis with wastewater concentrate feed : Fouling process considerations. J. Memb. Sci. 542, 233–244. https://doi.org/10.1016/j.memsci.2017.08.022

Shi, Y., Zhang, M., Zhang, H., Yang, F., Tang, C.Y., Dong, Y., 2021. Recent development of pressure retarded osmosis membranes for water and energy sustainability: A critical review. Water Res. 189, 116666. https://doi.org/10.1016/j.watres.2020.116666

Son, M., Park, H., Liu, L., Choi, Hyeongyu, Kim, J.H., Choi, Heechul, 2016. Thin-film nanocomposite membrane with CNT positioning in support layer for energy harvesting from saline water. Chem. Eng. J. 284, 68–77. https://doi.org/10.1016/j.cej.2015.08.134

Song, W., Li, Z., Ding, Y., Liu, F., You, H., Qi, P., Wang, F., Li, Y., Jin, C., 2018. Performance of a novel hybrid membrane bioreactor for treating saline wastewater from mariculture: Assessment of pollutants removal and membrane filtration performance. Chem. Eng. J. 331, 695–703. https://doi.org/10.1016/j.cej.2017.09.032

Song, W., You, H., Li, Z., Liu, F., Qi, P., Wang, F., Li, Y., 2017. Membrane fouling mitigation in a moving bed membrane bioreactor combined with anoxic biofilter for treatment of saline wastewater from mariculture. Bioresour. Technol. 243. https://doi.org/10.1016/j.biortech.2017.07.092

Sun, Y., Tian, J., Zhao, Z., Shi, W., Liu, D., Cui, F., 2016. Membrane fouling of forward osmosis (FO) membrane for municipal wastewater treatment: A comparison between direct FO and OMBR. Water Res. 104, 330–339. https://doi.org/10.1016/j.watres.2016.08.039

Tang, C.Y., She, Q., Lay, W.C.L., Wang, R., Fane, A.G., 2010. Coupled effects of internal concentration polarization and fouling on flux behavior of forward osmosis membranes during humic acid filtration. J. Memb. Sci. 354, 123–133. https://doi.org/10.1016/j.memsci.2010.02.059

Thorsen, T., Holt, T., 2009. The potential for power production from salinity gradients by pressure retarded osmosis. J. Memb. Sci. 335, 103–110. https://doi.org/10.1016/j.memsci.2009.03.003

Vinardell, S., Astals, S., Jaramillo, M., Mata-Alvarez, J., Dosta, J., 2021. Anaerobic membrane bioreactor performance at different wastewater pre-concentration factors: An experimental and economic study. Sci. Total Environ. 750, 141625. https://doi.org/10.1016/j.scitotenv.2020.141625

Vinardell, S., Astals, S., Mata-Alvarez, J., Dosta, J., 2020. Techno-economic analysis of combining forward osmosis-reverse osmosis and anaerobic membrane bioreactor technologies for municipal wastewater treatment and water production. Bioresour. Technol. 297, 122395. https://doi.org/10.1016/j.biortech.2019.122395

Wan, C.F., Chung, T.S., 2015. Osmotic power generation by pressure retarded osmosis using seawater brine as the draw solution and wastewater retentate as the feed. J. Memb. Sci. 479, 148–158. https://doi.org/10.1016/j.memsci.2014.12.036

Wang, X., Chang, V.W.C., Tang, C.Y., 2016a. Osmotic membrane bioreactor (OMBR) technology for wastewater treatment and reclamation: Advances, challenges, and prospects for the future. J. Memb. Sci. 504, 113–132. https://doi.org/10.1016/j.memsci.2016.01.010

Wang, X., Chen, Y., Yuan, B., Li, X., Ren, Y., 2014. Impacts of sludge retention time on sludge characteristics and membrane fouling in a submerged osmotic membrane bioreactor. Bioresour. Technol. 161, 340–347. https://doi.org/10.1016/j.biortech.2014.03.058

Wang, X., Wang, C., Tang, C.Y., Hu, T., Li, X., Ren, Y., 2017. Development of a novel anaerobic membrane bioreactor simultaneously integrating microfiltration and forward osmosis membranes for low-strength wastewater treatment. J. Memb. Sci. 527, 1–7. https://doi.org/10.1016/j.memsci.2016.12.062

Wang, X., Zhao, Y., Yuan, B., Wang, Z., Li, X., Ren, Y., 2016b. Comparison of biofouling mechanisms between cellulose triacetate (CTA) and thin-film composite (TFC) polyamide forward osmosis membranes in osmotic membrane bioreactors. Bioresour. Technol. 202, 50–58. https://doi.org/10.1016/j.biortech.2015.11.087

Xu, X., Zhang, H., Gao, T., Wang, Y., Teng, J., Lu, M., 2020. Customized thin and loose cake layer to mitigate membrane fouling in an electro-assisted anaerobic forward osmosis membrane bioreactor (AnOMEBR). Sci. Total Environ. 729, 138663. https://doi.org/10.1016/j.scitotenv.2020.138663

Yip, N.Y., Elimelech, M., 2011. Performance limiting effects in power generation from salinity gradients by pressure retarded osmosis. Environ. Sci. Technol. 45, 10273–10282. https://doi.org/10.1021/es203197e

Yuan, B., Wang, X., Tang, C., Li, X., Yu, G., 2015. In situ observation of the growth of biofouling layer in osmotic membrane bioreactors by multiple fluorescence labeling and confocal laser scanning microscopy. Water Res. 75, 188–200. https://doi.org/10.1016/j.watres.2015.02.048

Zaviska, F., Chun, Y., Heran, M., Zou, L., 2015. Using FO as pre-treatment of RO for high scaling potential brackish water: Energy and performance optimisation. J. Memb. Sci. 492, 430–438. https://doi.org/10.1016/j.memsci.2015.06.004

Table Captions

Table 1 TOC, NH_4^+-N, TN and TP concentrations in the influent, sludge supernatant and FO permeate and their removal rates (average ± standard deviation from triple measurements) in FO-MBR and PRO-MBR.

Table 2 The specific energy consumption of FO and PRO.

Table 3 Biovolume of the foulants on the fouled FO membranes in PRO-MBR and FO-MBR (calculated by PHLIP). [a]

Table 4 Performance comparison between the FO-MBR and the PRO-MBR.[a]

Figure Captions

Figure 1 Water flux profiles in PRO-MBR and FO-MBR with different membrane orientations (i.e., AL-DS and AL-FS).

Figure 2 Power density profiles of PRO-MBR operated in different membrane orientations (i.e., AL-DS and AL-FS).

Figure 3 SEM images (left) and EDS spectra (right) of the fouled FO membranes in the PRO-MBR and FO-MBR.

Figure 4 CLSM images of the fouled FO membranes in different membrane orientations in the PRO-MBR and FO-MBR (the cyan, blue, green and red colors represent α-D-glucopyranose, β-D-glucopyranose, proteins, and microbial cells, respectively).

Figure 5 Normalized fluxes of the fouled FO membranes in the PRO-MBR and FO-MBR before and after physical cleaning.